Turkish Journal of Electrical Engineering & Computer Sciences

http://journals.tubitak.gov.tr/elektrik/

Research Article

Turk J Elec Eng & Comp Sci
(2018) 26: 442 – 453

doi:10.3906/elk-1412-119

Improving the incremental conductance algorithm for two-stage grid-connected photovoltaic systems

Mehmet Ali ÖZÇELİK[1], **Ahmet Serdar YILMAZ**[2,*]

[1]Department of Electricity and Energy, Vocational School of Technical Sciences, Gaziantep University, Gaziantep, Turkey

[2]Department of Electrical & Electronics Engineering, Faculty of Engineering, Kahramanmaraş Sütçü İmam University, Kahramanmaraş, Turkey

Received: 20.12.2014 • **Accepted/Published Online:** 24.01.2016 • **Final Version:** 26.01.2018

Abstract: Efficiency of solar photovoltaic generation plants depends not only on internal operational conditions but also on external atmospheric conditions. Total efficiency is influenced by various weather conditions such as cloudiness, temperature, and irradiation. In order to generate maximum energy, photovoltaic (PV) arrays should be operated at their maximum power point (MPP), varying external factors like partial shading and surface temperature and amount of radiation coming from the sun. In modern PV systems, maximum power point trackers (MPPTs) have been used in order to reach the MPP, changing with the factors given above. MPPT units are implemented to control DC-DC converters that are connected to terminals of PV arrays. MPPTs operate according to some algorithms to reach the maximum power level in various conditions. This study presents a new modification of the incremental conductance (IncCond) algorithm, one of the best-known algorithms, to improve total efficiency of solar energy conversion systems. The proposed modified algorithm is able to catch the new MPP quickly compared to the conventional type and oscillations are also decreased, reaching a new operating point.

Key words: DC-DC converters, incremental conductance algorithm, maximum power point tracker, photovoltaic systems

1. Introduction

Maximum power point tracker (MPPT) systems have been used in photovoltaic (PV) power conversion systems because they have advantageous effects on overall efficiency. Recent studies about PV systems have focused on minimizing the costs and maximizing the conversion efficiency [1]. New methods and algorithms have been developed or modified to generate electrical power at maximum efficiency and minimum losses from solar cells. Solar cells have nonlinear characteristics and behave dependently on the current source. Voltage and current of solar cells change depending on irradiation and temperature [2]. Therefore, a MPPT control scheme requires variable temperature and solar irradiation conditions. MPPTs are improved to capture the maximum power level in different atmospheric conditions [3]. So as to maximize the conversion efficiency from solar arrays, the PV system should be operated at its MPP [4]. I-V and P-V characteristics of solar panels used in this study are given in Figure 1. As can be seen from Figure 1, solar irradiation increases the current and power coming from the solar panel under different test conditions.

*Correspondence: a.s.yilmaz@gmail.com

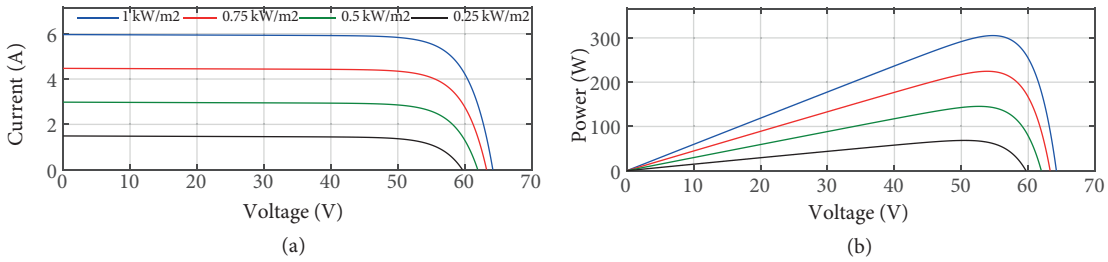

Figure 1. I-V and P-V characteristics of considered solar cell module.

The most important drawback of PV systems is the low-efficiency problem during power generation. Connection losses and shading on solar panels also cause an extra drop in the total efficiency. In addition to this, the angle of solar radiation and the temperature of both ambiance and panel surfaces also affect the total efficiency. Hence, PV systems should be operated at their MPP to improve total efficiency. MPPT algorithms should be applied to reach the MPP level in various conditions. Hence, it is possible to produce maximum power from PV systems. MPPT algorithms control DC-DC converters so as to track variable voltage and current among the panel and load. MPPT designs deal with converter type and algorithm. The selection of suitable converter type is a significant issue for MPPT design. Buck, boost, and buck-boost types are mostly preferred. Boost converters require more inductance than buck converters to achieve the same ripple of inductor current. In this type of converter, the current of the inductor is much less than that of buck converters. However, buck converters require larger and more expensive input capacitors than the boost type to even the discontinuous input current from the solar array. The polarity of output voltage of the buck/boost type varies. Hence, several converter types have been tested and suggested in the literature. In addition to the well-known buck, boost, and buck-boost types, second-generation converters such as SEPIC [5,6] and CUK [7,8] are used in this field as well as isolated flyback and forward [9] type converters used when higher voltage conversion is required. Furthermore, previous studies suggested various control methods for MPPT design. Fuzzy logic [10], digital signal processing controllers [11], field programmable gate array controllers [12,13], and parallel processing topology [14] are some of the important methods and controllers. To reach the MPP faster, several algorithms such as perturbation and observation [15,16], incremental conductance (IncCond), look-up table, current control loop [17], constant voltage, and Takagi–Sugeno fuzzy [18] were proposed and applied.

This study focuses on an optimization of the IncCond algorithm. The conventional IncCond algorithm is used with constant iteration step size. Therefore, its decision-making speed increases in proportion to the step size of error. However, a higher step size reduces the efficiency of the MPPT. This difficulty causes more power losses and complicates the control actions. Therefore, some calculation procedures of the conventional IncCond algorithm need to be modified. The proposed modification in this study is variable step size. The common grid-connected PV system consists of solar modules, a step-up DC-DC converter, and a DC-AC converter [19]. The proposed algorithm is simulated in grid-connected energy conversion systems including a solar panel, a DC-DC converter, and a DC-AC inverter as given in Figure 2.

2. Equivalent diagram and modeling of solar cells

Solar cells behave as a diode that has a PN junction. When sunlight falls on a cell, photo power acts like a forward diode on a large surface and generates electrical energy. As a result of sunlight hitting the cell, a potential difference and current flow occur. The current expression is given in Eq. (1).

$$I = I_{PH} - I_S \times \left\{ \exp\left[\frac{q}{A \times k \times T} (V + I \times R_L) \right] - 1 \right\} - \frac{(V + I \times R_S)}{R_{SH}} \quad (1)$$

Here, I_{PH}, I_S, R_L, Rs, R_{SH}, V, and I are photocurrent, saturation current, load resistance, series equivalent circuit resistance, parallel equivalent circuit resistance, output voltage, and load current, respectively. The equivalent circuit diagram for a solar cell is shown in Figure 3 [20].

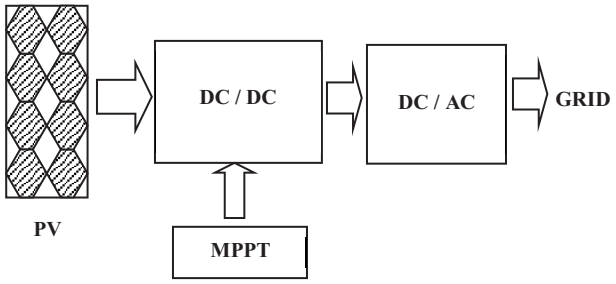

Figure 2. Conventional PV energy conversion system.

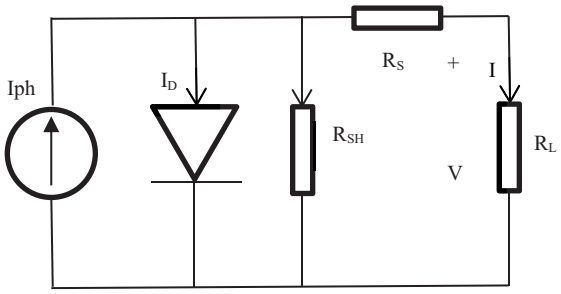

Figure 3. Equivalent circuit diagram for solar cells.

PV panels combined with series and parallel-connected solar cells electrically connect a current source, series and parallel resistances, and parallel diodes. The relation between the voltage and current of solar cells exposes I-V and P-V characteristics. These two characteristics give important clues regarding which conditions are required in order to obtain power from the panel to reach its maximum level. Obtaining maximum power and reaching the highest efficiency level from panels are important research topics. Solar panels act like a current source from a certain point onward, while they act like a voltage source. The current that can be obtained from a solar panel is fixed even in the case of a short circuit. This parameter is given in the datasheet of the panel along with the plate value of the panel. It is necessary to obtain maximum power from PV panels in different irradiation conditions. The electrical parameters of the PV array used in this study are given in the Table.

Table. Electrical characteristics of PV panel (SunPower SPR-305-WHT).

Module specifications under STC	Parameters
Open-circuit voltage (Voc)	64.2 V
Short-circuit current (Isc)	5.96 A
Voltage at Pmax (Vmp)	54.7 V
Current at Pmax (Imp)	5.58 A
Number of series-connected modules per string	5
Number of parallel strings	66

3. Essentials of incremental conductance algorithm

As shown in Figure 1, solar cells have two main characteristics. The P-V (power-voltage) curve illustrates the generated power depending on output voltage. The highest point of that curve is also called the MPP. At that point, the power derivative with respect to voltage is zero. The IncCond algorithm seeks the MPP during variable operating conditions continuously. The algorithm is summarized by Eq. (2).

$$\frac{dP}{dV} = \frac{d(VI)}{dV} = I + V \times \frac{dI}{dV} = 0, \text{ at the MPP} \quad (2)$$

Eq. (3) is derived from Eq. (2) as follows.

$$\frac{I}{V} = -\frac{dI}{dV} \tag{3}$$

The left-hand side of Eq. (3) represents the opposite of the solar array's instantaneous conductance and the right-hand side represents its incremental conductance. As a consequence, the method requires the application of a repeated perturbation of the voltage value, until the next condition [21,22] occurs, as in Eq. (4).

$$\frac{I_k}{V_k} = -\frac{I_k - I_{k-1}}{V_k - V_{k-1}} \tag{4}$$

Here, the subscripts k and $k-1$ refer to two sequential samples of the PV voltage and current values. The conventional IncCond algorithm [23] is shown Figure 4. The equations at the MPP are as follows:

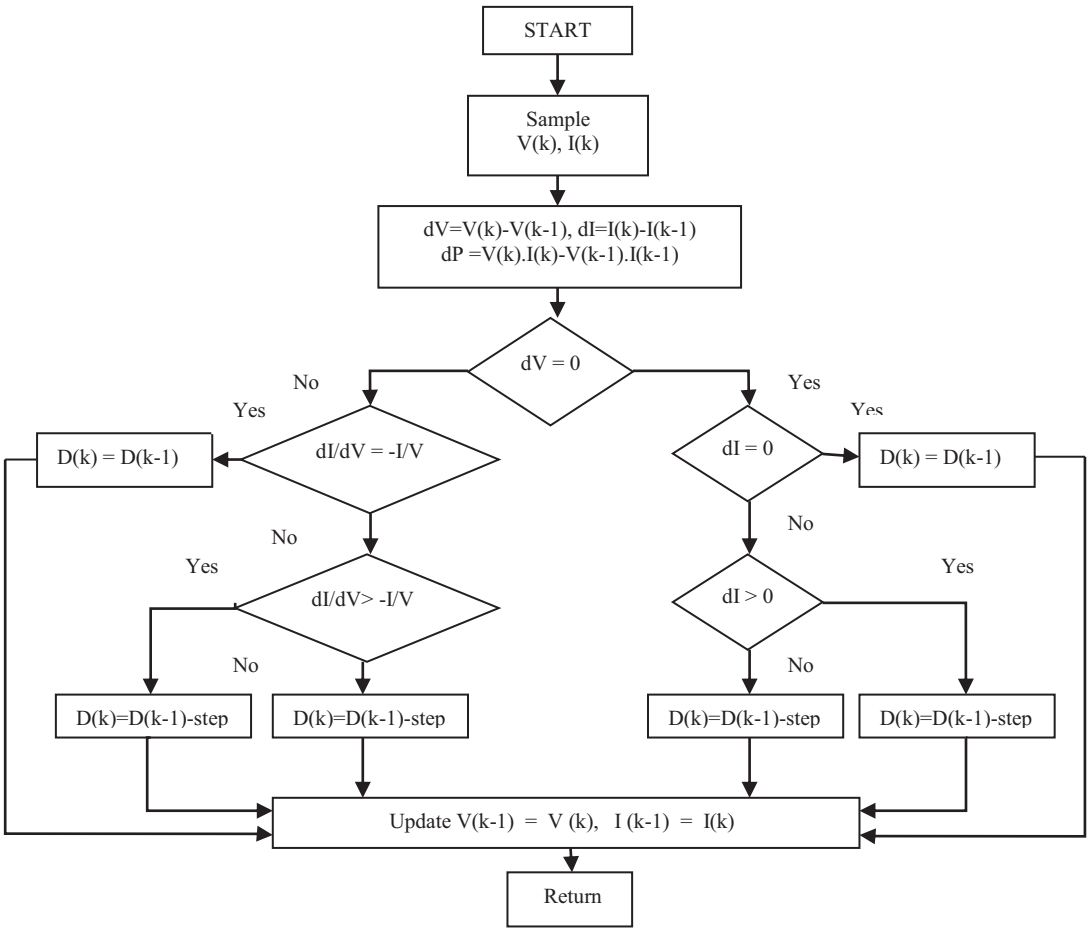

Figure 4. Flowchart of the conventional IncCond algorithm.

$$\frac{dI}{dV} = -\frac{I}{V}; \quad \left(\frac{dP}{dV} = 0\right), \text{ at MPP} \tag{5a}$$

$$\frac{dI}{dV} > -\frac{I}{V}; \quad \left(\frac{dP}{dV} > 0\right), \text{ left of MPP} \tag{5b}$$

$$\frac{dI}{dV} < -\frac{I}{V}; \quad \left(\frac{dP}{dV} < 0\right), \text{ right of MPP} \tag{5c}$$

Basically, Eq. (2) is repeated in Eq. (5a). This equation that defines the derivative of current with respect to voltage should be zero at the MPP. The main goal of the algorithm is to catch that point in different conditions. Solar cells have several P-V curves depending on temperature and irradiation level, as seen in Figure 1. Therefore, the MPP may change continuously and the algorithm always has to find it. Eqs. (5b) and (5c) define the inequalities for the left and right side of the MPP. On the left side of the MPP, the derivative of power according to voltage is positive and voltage should be increased. After that, the derivation should be recalculated as it reaches zero. Similarly, on the right side of the MPP, the derivation is negative and the algorithm tries to find the MPP by decreasing the voltage until it reaches zero. When the MPP is reached, the MPPT continues to operate at this point until another variation occurs in the current. The increasing of iteration steps decides how fast the MPP is tracked and reached. Faster tracking can be achieved with large increments, but the system cannot work stably and some oscillations around the MPP may occur.

4. Proposed incremental conductance algorithm modification

In the proposed algorithm, instead of a constant step coefficient, ΔP was adopted as in Eq. (6) in order to attain the MPP.

$$\Delta P = V(k) \times I(k) - V(k-1) \times I(k-1) \tag{6}$$

In other words, change of power generates ΔP and it provides a faster way for identifying the MPP. $\Delta P = 0$ means no iteration has been performed with regards to duty cycle changing and the ripple was minimized. Thus, a parallel coefficient was provided for power change to faster identify the MPP. In addition, at the MPP, $\frac{dI}{dV} + \frac{I}{V} = 0$ and no iteration is performed. Conductance error is ε of the present measurement and the recorded conductance G_{mpp} is characterized by $\varepsilon = i/v - G_{mpp}$ [20]. This ε value can generate ripple under variable solar irradiation [24]. The ripple causes power loss. If the absolute value of $\frac{dI}{dV} + \frac{I}{V}$ is smaller or equal to ε, the step of the duty cycle will be reset ($\Delta P = 0$), which means that D(k) = D(k–1) and so ripple will be eliminated. The flowchart of the proposed algorithm is shown in Figure 5. The flowchart in Figure 5 was designed in order to prevent ripple emerging during attempts to identify the MPP of the IncCond algorithm and to more quickly identify this point following significant power changes.

In this approach, ΔP denotes power change. When the panel and duty cycle of the DC-DC converter $[D(k)]$ is increased or decreased in accordance with this power change, it is found in the simulation results that ripple is reduced and $D(k)$ at the MPP is identified sooner. In the case of no power change, $\Delta P = 0$ or $abs(\frac{dI}{dV} + \frac{I}{V}) \leq \varepsilon$, no iteration is performed. In this case, ripple around the MPP under variable solar irradiation is eliminated, thus improving the algorithm. When power change increases, the iteration coefficient increases. Otherwise, the iteration coefficient decreases. At the left side of the MPP, if $D(k)$ increases, power increases, and if $D(k)$ decreases, power decreases, too. Conversely, at the right side of the MPP, when $D(k)$ increases, power will decrease, and when $D(k)$ decreases, power will increase. Therefore, when the duty cycle is changed, if there is an increase in power, change in the same way should be maintained (a step that equals absolute value ΔP should be added). If there is a decrease in power, change should be continued in an inverse way (ΔP should be subtracted). Thus, a more determined algorithm is developed. As seen from Figure 2, the MPPT is a power tracking system that enables us to obtain maximum power from PV panels. In the MPPT block, the DC-DC converter is controlled by the IncCond algorithm by tuning the duty cycle. As a result of this, the maximum power level from the PV panel is reached. In this configuration, depending on the atmospheric changes, the changing duty cycle controls the DC-DC and DC-AC converters to reach the MPP. The studied system is

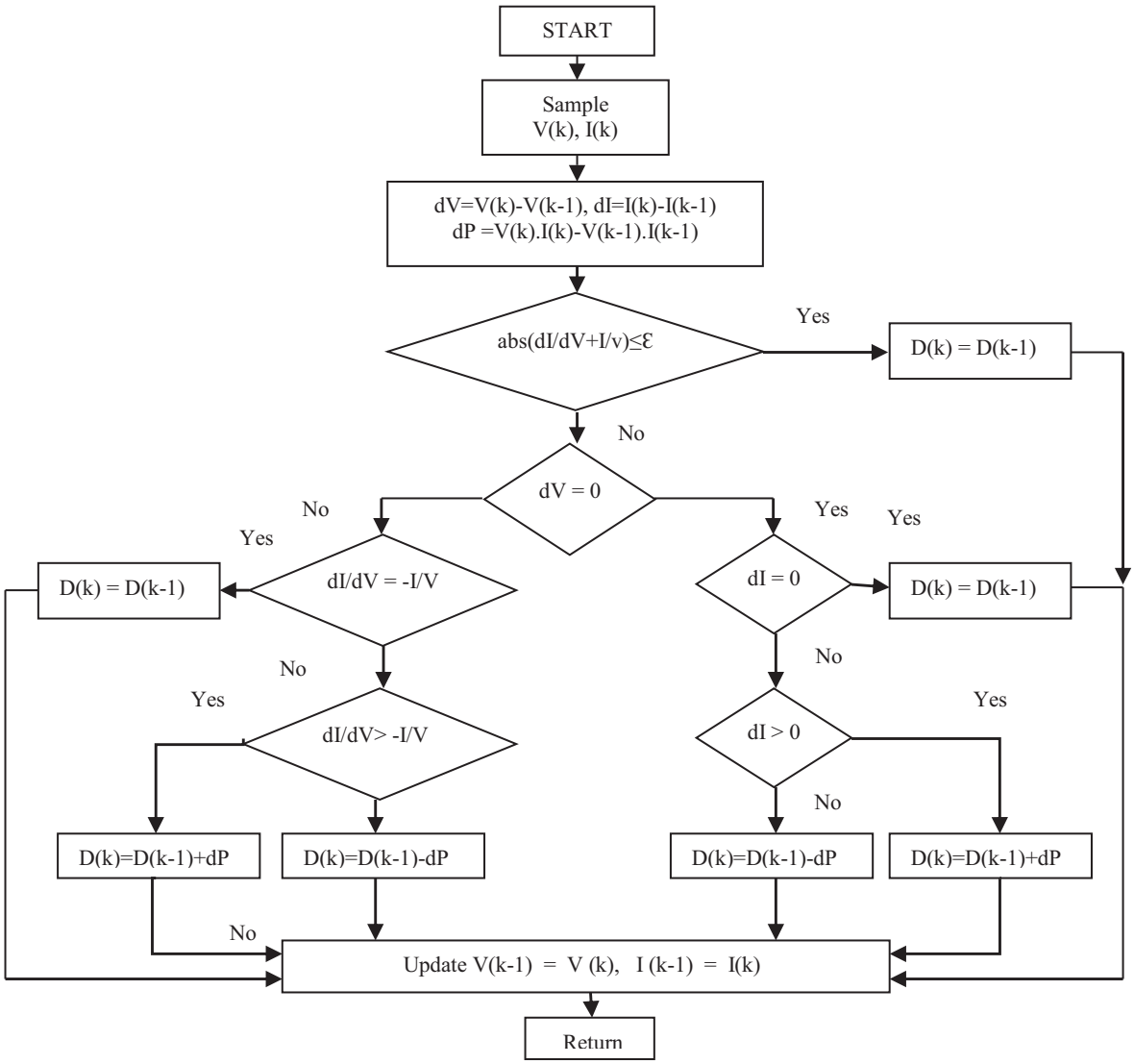

Figure 5. Flowchart for proposed IncCond algorithm.

simulated by using the Simulink/Simpower system toolbox. In the simulations, the proposed controller was modeled using the MATLAB Function Block. A MATLAB code was also written and added to the MATLAB Function Block.

5. Test results

In the simulations, three cases are considered to compare both algorithms. In the first case, outputs of the DC-DC converter (DC side) are considered when insolation decreases. In the second, the same parameters are also considered when insolation increases and decreases. In the last case, outputs of the inverter (AC side) are considered when insolation increases or decreases. The block scheme for both this case and the previous case is given in Figure 6.

The block scheme is an average model of a PV array connected to a 35-kV grid via two DC-DC boost converters and a single three-phase voltage source converter (VSC). The two MPPT controllers based on the

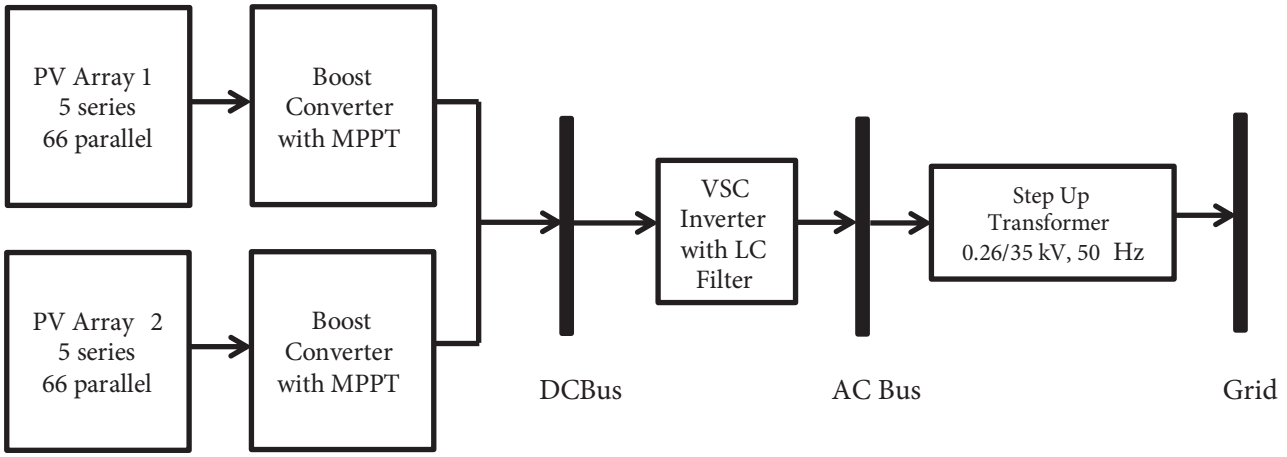

Figure 6. Schematic block diagram of simulated systems.

IncCond technique are implemented by means of a MATLAB function block that generates embeddable C code. The model contains two average boost converter models, which increase the array voltage to 500 V DC. The boost converter produces an output voltage that is greater than or equal to the input voltage; as the duty ratio (D) of the switch approaches unity, the output voltage goes to infinity according to Eq. (7) [25]. V_o is the output voltage of the boost converter and V_s is the output of the PV array in this expression.

$$V_o = \frac{V_s}{1 - D} \tag{7}$$

η is efficiency of the boost converter and the maximum duty ratio is given by Eq. (8).

$$D_{\max} = 1 - \frac{V_{s(\min)} \times \eta}{V_o} \tag{8}$$

The boost converter voltage is increased from 273.5 V to 500 V. This converter uses a MPPT system that automatically varies the duty cycle in order to generate the required voltage to extract maximum power. The average model of the VSC converts the 500 V DC to 260 V AC and keeps unity power factor. The control of the VSC system uses two control loops: an external control loop, which regulates the DC link voltage to ± 250 V, and an internal control loop, which regulates Id and Iq grid currents. Id and Iq current references are the outputs of the DC voltage regulator unit. Voltage outputs of the controller are converted to three modulating signals U_{ref} by using pulse width modulation (PWM). The control system uses a sample time of 100 μs for voltage and current control units to synchronize the phase-locked loop. Additionally, pulse generators of the DC-DC converter and VSC utilize a sample time of 1 μs in order to get appropriate resolution of PWM signals. The block diagram for VSC control is shown in Figure 7 [26].

Figure 8 shows the input voltage of the VSC control unit, output Vref of the VSC, and Va grid voltage under various irradiation conditions.

To reach a balance of flow between the AC and DC of the VSC, V_{dc} reference is kept on the inverter side. The reactive power reference is set to zero, which is unity power factor, but in line with the system requirements it could be changed.

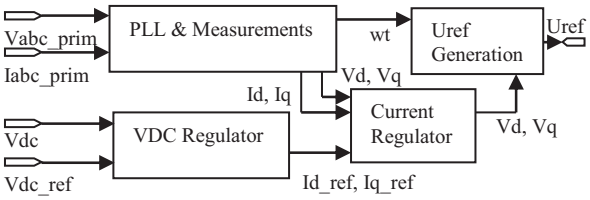

Figure 7. VSC control block diagram.

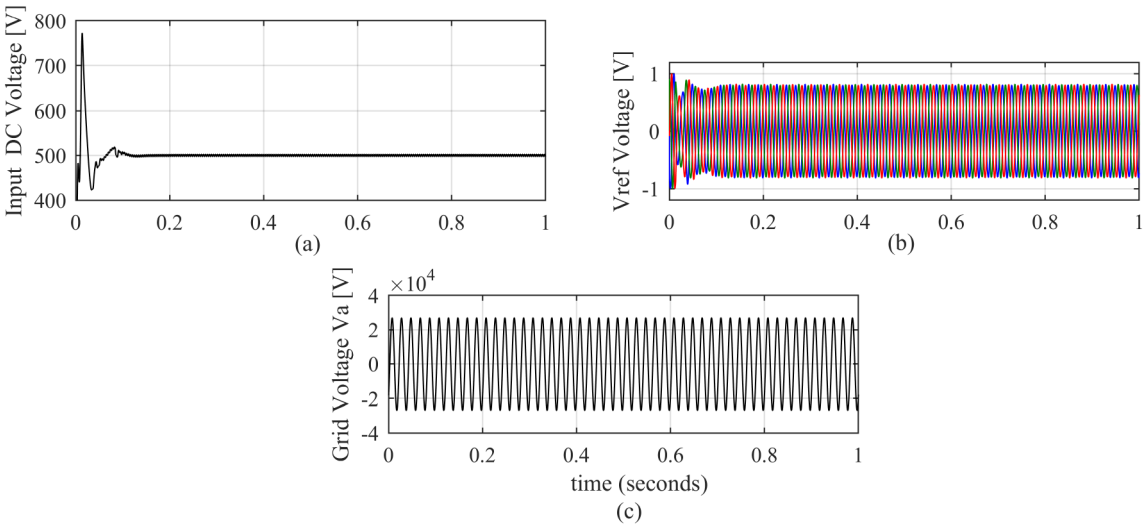

Figure 8. (a) Input voltage of VSC control unit, (b) output Vref of VSC, (c) Va grid voltage.

5.1. Results for case I

Results obtained from the modeling in MATLAB/Simulink are presented in this section. Solar irradiation is around 1000 W/m^2 at the starting point. Irradiation is decreased to about 980 W/m^2 linearly until 0.5 s. In this case, a linear decrease was observed in the system, which is exposed to a radiation rate of about 1000 W/m^2 for 0.5 s, and the radiation decreased to nearly 980 W/m^2. In view of this change, it can be considered as a slow, classical method and responses of identical systems operated by the modified method were compared. Power and current responses are compared in Figures 8 and 9. It can be seen from the results in Figures 9 and 10 that oscillations were eliminated by the proposed method. The current is changed smoothly according to insolation. Smoothing in the changing of the current also provides less loss. In the steady state, this dramatically reduces ripples in PV power and current compared to continuous perturbations caused by IncCond-type algorithms.

5.2. Results for case II

In this simulation, solar irradiation is 1150 W/m^2 at the starting point. It is increased to 1250 W/m^2 until t = 2.65 s. After that, it is decreased to under 950 W/m^2 until t = 2.7 s. Finally, solar irradiation is increased again to 1000 W/m^2 linearly until the end of the simulation, as seen in Figure 11. Compared with the results of power changing in Figure 8, the modified algorithm increased power demand from the solar arrays and also oscillations were eliminated. Therefore, more power and less loss can be obtained from the PV arrays by using the modified algorithm.

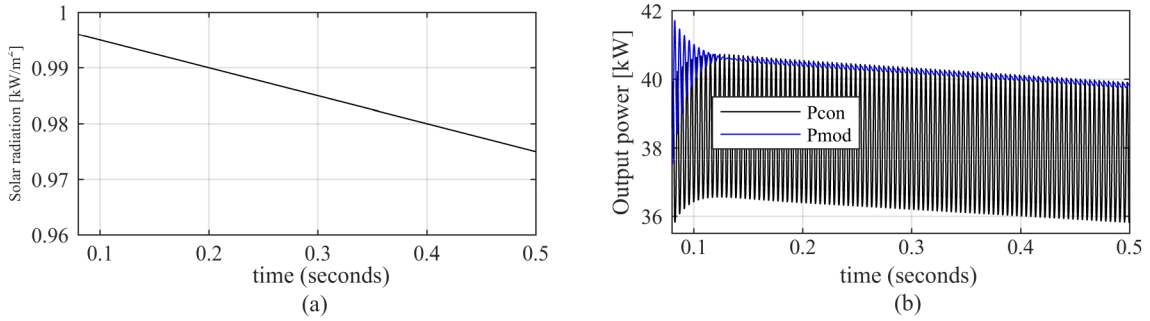

Figure 9. (a) Solar radiation, (b) output power of DC side for both algorithms in case I.

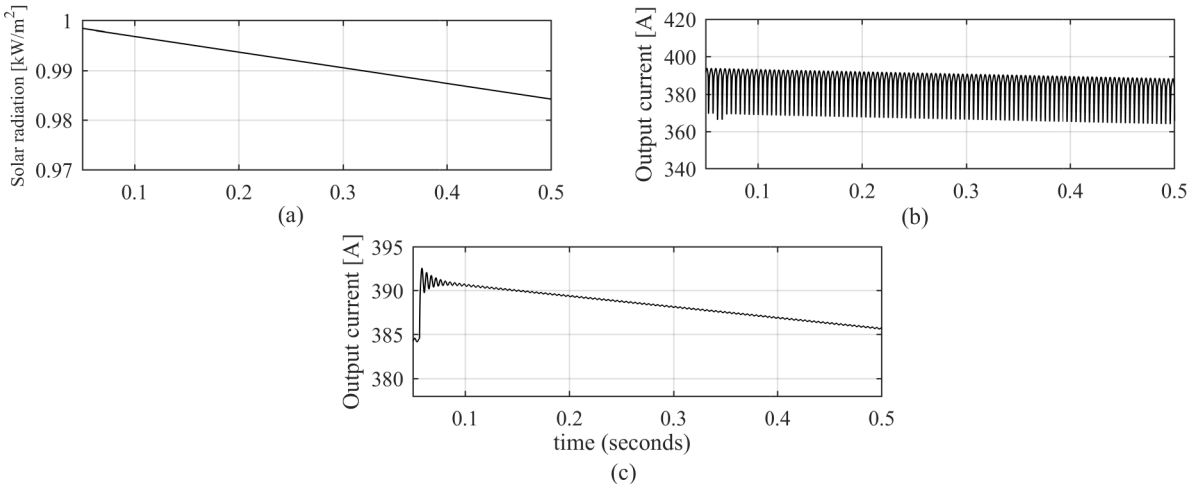

Figure 10. (a) Changing of solar radiation and output current of DC side for (b) conventional and (c) modified IncCond algorithms in case I.

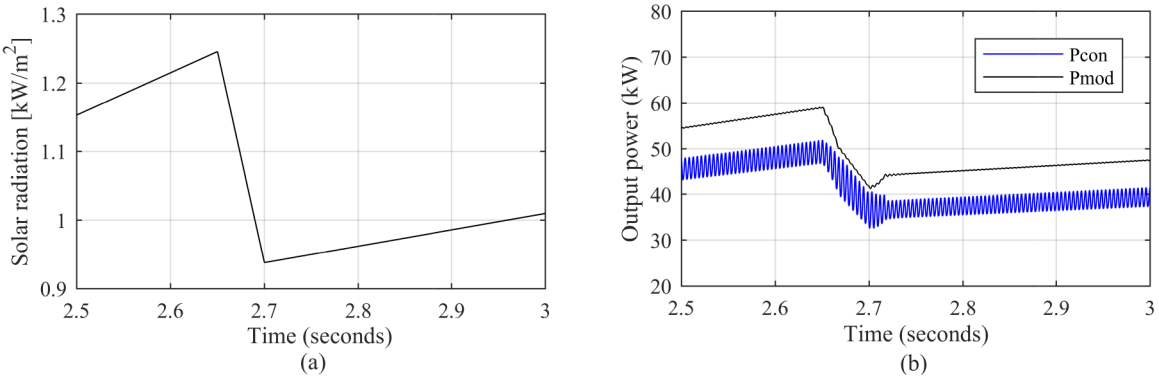

Figure 11. (a) Changing of solar radiation and (b) output power of DC side for both algorithms in case II.

5.3. Results for case III

In this case, only AC side waveforms are considered and given in the following figures.

In this simulation case, solar insolation is increased from 1000 W/m^2 to 1050 W/m^2 during the first 0.7 s. Then it is decreased to 850 W/m^2 and increased to 1150 W/m^2 again, as seen in Figure 12. In the proposed algorithm, generated power is increased by about 20% compared to the conventional algorithm. The increase

in current can be seen clearly in Figure 13. This figure illustrates the sinusoidal current waveform to the grid. Voltage waveforms of both algorithms are given in Figure 14. It can be seen from the results of these three cases that the modified IncCond algorithm reaches the MPP in less time than the conventional IncCond algorithm in this process. In addition, the modified IncCond algorithm produces fewer ripples than the conventional IncCond algorithm under various solar insolation conditions and the modified IncCond algorithm is more efficient than

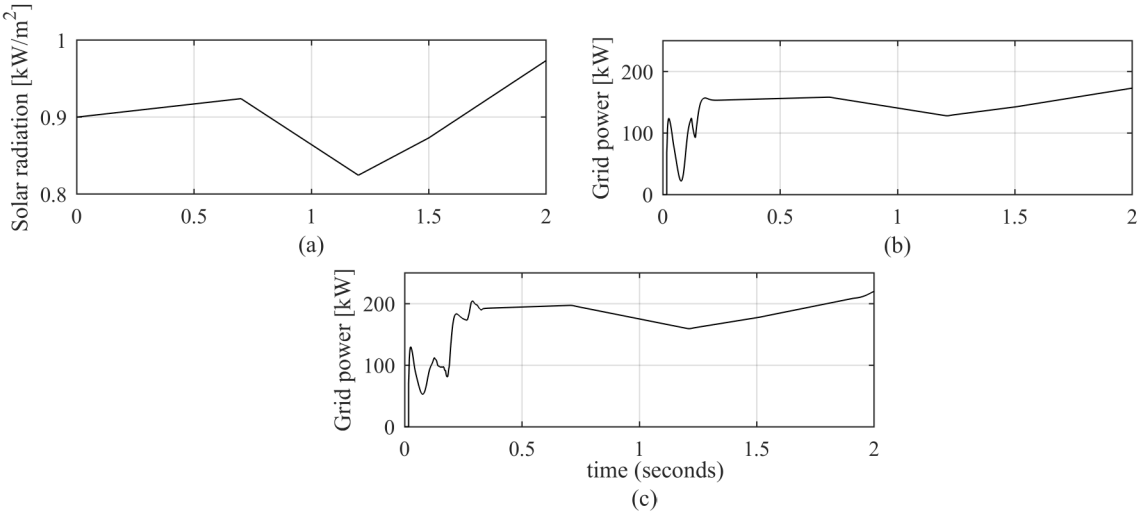

Figure 12. (a) Changing of solar radiation (W/m^2) and grid power (kW) for (b) conventional and (c) modified IncCond algorithms in case III.

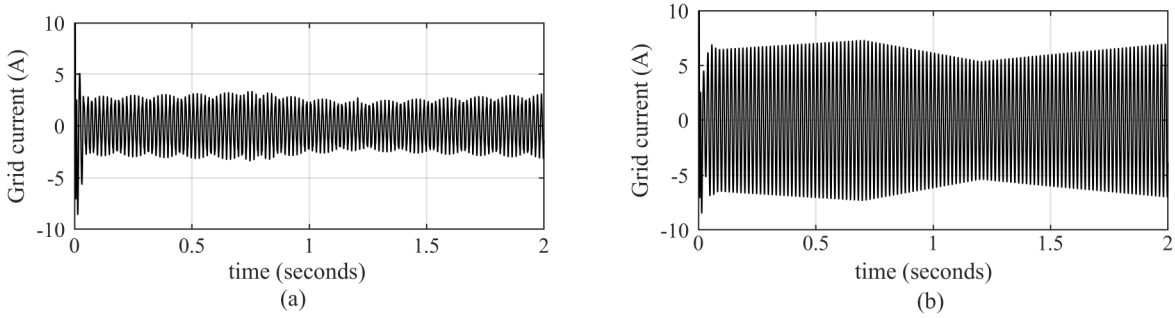

Figure 13. Total current to grid for (a) conventional and (b) modified IncCond algorithms in case III.

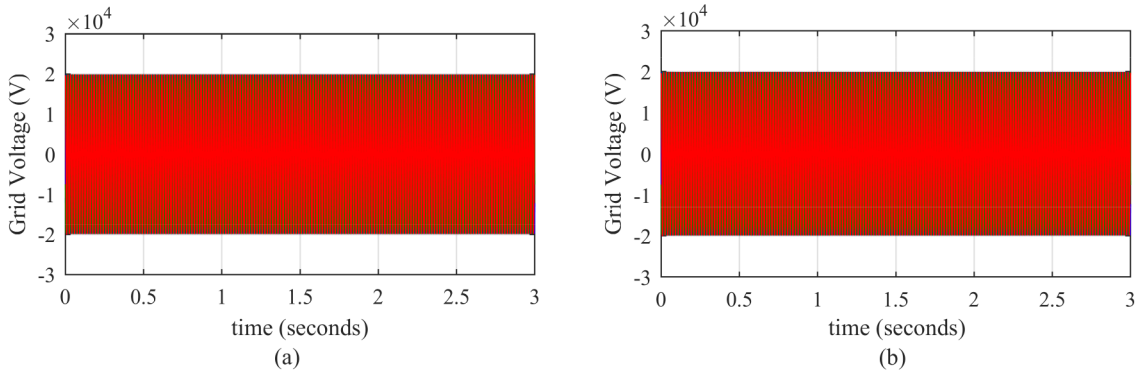

Figure 14. Total voltage to grid for (a) conventional and (b) modified IncCond algorithms in case III.

the conventional IncCond algorithm. With the conventional IncCond algorithm, ripples occur and the MPP is attained slightly later. Particularly, as shown in the figures, ripples in power and current continue for a specific period of time. These ripples affect the total efficiency of the system negatively, too. Losses may be encountered due to changing parameters as a result of ripples. As these results also suggest, ripple, power loss, and slow response persist in conventional methods. These problems bring disadvantages because they affect the total efficiency of the panel and extend MPPT identification time.

6. Conclusions

PV systems have low efficiency in general. System efficiency involves much equipment and many parameters in the system. Efficiency of a single solar cell may differ from that of the panels that constitute these cells. Problems during installation negatively affect panel efficiency. There are also other factors such as panel angle, obstruction by high buildings, or cloudy weather conditions that cause total or partial shadowing and thus decrease total efficiency. Additionally, software and hardware problems in the MPPT decrease efficiency. Switching losses in the converter circuit may also have a negative influence on total efficiency. Slow response rate of the algorithm and, as stated in this study, occurrence of ripples are also important problems under changing solar insolation conditions. These factors force us to improve the algorithm. This study focuses on improving the algorithm and eliminating ripple problems in the IncCond algorithm. When variability increases as a result of factors such as partial shadowing and cloudy weather, these ripples affect the performance of the system particularly badly. In order to increase the efficiency of system, it is suggested that the algorithm be improved accordingly. It is also possible to suggest that changes to the algorithm will create no difficulties in terms of hardware, which makes it suitable for experimental purposes. An improved IncCond algorithm is used to modulate the duty cycle of the boost DC-DC converter and inverter, and thus the tracking speed increased. It is concluded that the proposed algorithm shows better performance than the conventional IncCond algorithm under changing conditions and it reduces the power losses.

References

[1] Wei X, Chaoxu M, Jianxun J. Novel linear iteration maximum power point tracking algorithm for photovoltaic power generation. IEEE T Appl Supercon 2014; 24: 0600806.

[2] Tey KS, Mekhilef S. Modified incremental conductance algorithm for photovoltaic system under partial shading conditions and load variation. IEEE T Ind Electron 2014; 61: 5384-5392.

[3] Hussein KH, Muta I, Hoshino T, Osakada M. Maximum photovoltaic power tracking: an algorithm for rapidly changing atmospheric conditions. IEE P-Gener Transm D 1995; 142: 59-64.

[4] Hohm D, Ropp ME. Comparative study of maximum point tracking algorithms using an experimental, programmable, maximum power point tracking test bed. In: Proceedings of the 28th IEEE Photovoltaic Specialists Conference; 15–22 September 2000; Anchorage, AK, USA. New York, NY, USA: IEEE pp. 1699-1702.

[5] Veerachary M. Power tracking for non-linear PV sources with coupled inductor SEPIC converter. IEEE T Aero Elec Sys 2005; 41: 1019-1029.

[6] Chiang SJ, Shieh HJ, Chen MC. Modeling and control of PV charger system with SEPIC converter. IEEE T Ind Electron 2009; 56: 4344-4353.

[7] Raiwan DC, Nayar CV. Analysis and design of a solar charge controller using CUK converter. In: AUPEC 2007 Power Engineering Conference; 9–12 December 2007; Perth, Australia. New York, NY, USA: IEEE. pp. 1-6.

[8] Safari A, Mekhilef S. Simulation and hardware implementation of incremental conductance MPPT with direct control method using CUK converter. IEEE T Ind Electron 2011; 58: 1154-1161.

[9] Vermulst BJD. Isolated high-efficiency DC/DC converter for photovoltaic applications. In: 38th Annual Conference on IEEE Industry Application Society; 25 October 2012; Montreal, Canada. New York, NY, USA: IEEE. pp. 25-28.

[10] Altas IH, Sharaf AM. A novel maximum power fuzzy logic controller for photovoltaic solar energy systems. Renew Energ 2008; 33: 388-399.

[11] Hua C, Lin J, Shen C. Implementation of a DSP-controlled photovoltaic system with peak power tracking. IEEE T Ind Electron 1998; 45: 99-107.

[12] Koutroulis E, Kalaitzakis K, Tzitzilonis V. Development of an FPGA based system for real-time simulation. J Microelectronics 2009; 40: 1094-1102.

[13] Mellit A, Rezzouk H, Messai A, Medjahed B. FPGA-based real time implementation of MPPT-controller for photovoltaic systems. Renew Energ 2011; 36: 1652-1661.

[14] Badawy MO, Yilmaz AS, Sozer Y, Husein I. Parallel power processing topology for solar PV applications. IEEE T Ind Appl 2014; 50: 1245-1255.

[15] Salas V, Olias E, Lazaro A, Barrado A. Evaluation of a new maximum power point tracker (MPPT) applied to the photovoltaic standalone systems. Sol Energy Mat Sol C 2005; 87: 807-815.

[16] Esram T, Chapman PL. Comparison of photovoltaic array maximum power point tracking techniques. IEEE T Energy Conver 2007; 22: 439-449.

[17] Goncalves WM, Alves RNC, da Fonseca Neto JV, Fonseca WAS. Current control loop for tracking of MPPT supplied for photovoltaic array. IEEE T Instrum Meas 2004; 53: 1304-1310.

[18] Sekhar PC, Mishra S. Takagi-Sugeno fuzzy-based incremental conductance algorithm for maximum power point tracking of a photovoltaic generating system. IET Renew Power Gen 2014;8: 900-914.

[19] Aranzazu DM, Cano JM, Fernando AS, V'azquez JR. Backstepping control of smart grid-connected distributed photovoltaic power supplies for telecom equipment. IEEE T Energy Conver 2015; 30: 1496-1504.

[20] Onat N. Recent developments in maximum power point tracking technologies for photovoltaic systems. Int J Photoenergy 2010; 2010: 245316.

[21] Mohamed AE, Zhengming Z. MPPT techniques for photovoltaic applications. Renew Sust Energ Rev 2013; 793-813.

[22] Nicola F, Giovanni P, Giovanni S, Massimo V. Power Electronics and Control Techniques for Maximum Energy Harvesting in Photovoltaic Systems. 1st ed. Boca Raton, FL, USA: CRC Press, 2013.

[23] Abdourraziq MA, Maaroufi M. A new variable step size INC MPPT method for PV systems. In: IEEE 2014 Multimedia Computing and Systems International Conference; 14–16 April 2014; Marrakesh, Morocco. New York, NY, USA: IEEE. pp 1563-1568.

[24] Weidong X, Dunford WG, Palmer RP, Capel A. Application of centered differentiation and steepest descent to maximum power point tracking. IEEE T Ind Electron 2007; 54: 2539-2549.

[25] Ishaque K, Salam Z. A review of maximum power point tracking techniques of PV system for uniform insolation and partial shading condition. Renew Sust Energ Rev 2013; 19: 475-488.

[26] Hart DW. Power Electronics. New York, NY, USA: McGraw-Hill, 2011.

[27] Banu IV, Istrate M, Machidon D, Pantelimon R. A study on anti-islanding detection algorithms for grid-tied photovoltaic systems. In: International Conference on Optimization of Electrical and Electronic Equipment; 22–24 May 2014; Bran, Romania. New York, NY, USA: IEEE. pp. 655-660.